Effect of substituents in sulfoxides on the enhancement of thermoelectric properties of PEDOT:PSS: experimental and modelling evidences

Qiang Zhu,[a] Erol Yildirim,[b] Xizu Wang,[a] Aung Ko Ko Kyaw,[a] Tao Tang,[a] Xiang Yun Debbie Soo,[a] Zicong Marvin Wong,[b] Gang Wu,[b] Shuo-Wang Yang*,[b] and Jianwei Xu*,[a,c]

Poly(3,4-ethylenedioxythiophene):poly(styrenesulfonate) (PEDOT:PSS), being the most popular conductive polymer, has been doped with various additives with the aim to improve its thermoelectric performance. Among all additives, dimethyl sulfoxide (DMSO) has been widely used for various treatments. In this work, we designed and synthesized a series of aliphatic- and aromatic-substituted sulfoxides as dopants to improve the thermoelectric properties of PEDOT:PSS. It was found that the substituents in sulfoxide played a vital role in controlling the thermoelectric properties. Sulfoxides with relatively longer alkyl chain and large phenyl groups increased the electrical conductivity of PEDOT:PSS to more than 200 S/cm compared to pristine PEDOT:PSS film. Sulfoxide with 4-nitrophenyl substituents, however, led to negligible changes in electrical conductivity but increased the Seebeck coefficient from 22 to 56 μV/K. In contrast, sulfoxide with 4-hydroxyphenyl substituents remarkably improved both the electrical conductivity and Seebeck coefficients, leading to a power factor of up to 69 μW m^{-1} K^{-2}, much higher than that of PEDOT:PSS film which was obtained by simply mixing with DMSO. Several simulation methods were used to evaluate various interactions between sulfoxides, PEDOT, and PSS to elucidate the mechanisms, revealing that the sulfoxide with 4-hydroxy phenyl groups possessed additional interaction with the PSS phase, while the sulfoxide with 4-nitrophenyl groups showed strong interaction with the PEDOT phase instead and hence disrupted electrical conductivity. Our findings would uncover the mechanism of electrical conductivity enhancement, providing a general strategy for designing promising alternative additives for PEDOT:PSS treatment and eventually achieving better thermoelectric properties.

Introduction

The practicality of converting waste heat into useful electrical energy has sparked the research on thermoelectric (TE) materials since the 1800s. With the increasing environmental problems attributable to energy production in recent years, there has been a huge demand in the search for an efficient TE material.[1-4] The efficiency of the TE material can be determined by the dimensionless figure of merit: $zT = (\sigma S^2)T/\kappa$, where σ is the electrical conductivity, S is the Seebeck coefficient, κ is the thermal conductivity, and T is the absolute temperature. The above equation to obtain zT indicates that a higher electrical conductivity and Seebeck coefficient will give a higher conversion efficiency; however, it has been proven very challenging to achieve high electrical conductivity and high Seebeck coefficient simultaneously due to their trade-off relationship.[5] In practice, the power factor PF = σS^2 is usually used to evaluate the TE performance. In order to achieve high-performance TE materials, various kinds of materials have been investigated systematically with the aim of maximizing and balancing the two parameters.

Traditionally, inorganic materials[6-13] such as Bi_2Te_3/Sb_2Te_3,[6] PbSeTe,[12] SiGe[13], *etc.* have been studied extensively and displayed high zT values of around 2.[14] These materials display impressive thermoelectric performance, but they possess intrinsic disadvantages such as toxicity, scarcity, high cost, restricted processability, and some of the materials do not function well for heat harvesting at ambient temperatures. Therefore, an alternative class of materials, conductive polymers (CPs) have been emerging as they possess low thermal conductivity, tuneable electrical conductivity, and relatively low cost. The commonly studied CPs include poly(3,4-ethylenedioxythiophene):poly(styrenesulfonate) (PEDOT:PSS),[15] polyaniline,[16-18] polythiophene,[18, 19] polypyrrole,[20] and polyacetylene.[21] Although the current performance of CPs cannot rival those of traditional inorganic TE counterparts, the TE performance for CPs has been improved by several orders over the years, showing very promising trends of zT values for the practical applications.[22-29]

Among all the CPs, PEDOT:PSS has been demonstrated as a champion CP owing to high electrical conductivity, water-processability, and commercial availability. In order to enhance its TE performance, several approaches have been widely examined. Firstly, PEDOT:PSS can be hybridized with different inorganic or organic nanomaterials.[30] This allows hybrid materials to tap on the advantageous properties of each component, such as electrical conductivity or Seebeck coefficient to offset each other's disadvantages to give an optimum thermoelectric performance.[15, 31-33] Unfortunately the functioning mechanism of this hybridization is not yet well understood despite recent efforts,[34] and thus far the highest zT obtained is 0.2.[35] Another challenge is the incompatibility of the two components as observed in many cases, where phase separation of each component leads to non-uniform films.[36] Secondly, PEDOT itself can be synthesized into nanostructures such as nanorods, nanofibers, or nanotubes to improve TE performance as compared to bulk CPs.[30,37] Nevertheless the fabrications of such nanostructures as well as scaling-up processes are challenging,

[a] *Institute of Materials Research and Engineering, A*STAR (Agency for Science, Technology and Research), 2 Fusionopolis Way, Innovis, #08-03, Singapore 138634, Singapore. Email: jw-xu@imre.a-star.edu.sg; yangsw@ihpc.a-star.edu.sg*
[b] *Institute of High Performance Computing, Agency for Science, Technology and Research, 1 Fusionopolis Way, #16-16 Connexis, Singapore 138632.*
[c] *Department of Chemistry, National University of Singapore, 3 Science Drive 3, Singapore 117543*

† Footnotes relating to the title and/or authors should appear here.

Electronic Supplementary Information (ESI) available: [details of any supplementary information available should be included here]. See DOI: 10.1039/x0xx00000x

limiting their applications. Lastly, surface modifications through secondary doping such as pre-mixing and post-treatment of the PEDOT:PSS film are also proven to be effective approaches. Various post-treatment methods of PEDOT:PSS have been extensively studied,[38, 39] and the main aim for the post treatment is to remove the insulating PSS segment from PEDOT:PSS. The common process is to immerse the film into various organic and mineral acids, organic solvents such as dimethyl sulfoxide (DMSO) and ethylene glycol (EG).[40, 41] Mineral acids and organic solvents as well as sequential acid and base post-treatments have been proven to increase the electrical conductivity of PEDOT:PSS by a few magnitudes, giving rise to a significant increase in power factor.[15, 40, 42] The highest *zT* so far was reported to be 0.4 by Pipe et al.[43]

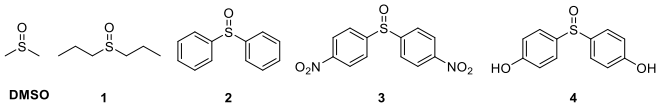

Figure 1. Chemical structures of DMSO and DMSO analogues

DMSO has been widely employed to dope PEDOT:PSS for electrical conductivity enhancement of up to 1000 S/cm. This high electrical conductivity is important in order to achieve good TE performance. The working mechanism for DMSO is to remove insulating polymer PSS from PEDOT:PSS.[44] We studied the mechanism of electrical conductivity enhancement of PEDOT:PSS with treatment of DMSO at the molecular level, demonstrating that DMSO dissolves the PSS shell to release the conductive PEDOT in the core for self-aggregation, resulting in phase separation of PEDOT and PSS by charge screening.[10] As such, it would be more interesting if we integrate some structural variables such as aromatic moieties with different functional groups into sulfoxides and investigate how the structural changes in sulfoxides affect the thermoelectric parameters such as electrical conductivity and Seebeck coefficient. Thus, it would give us an insight on how to design and select an effective additive to treat PEDOT:PSS to achieve a better performance. In order to verify this hypothesis, a series of sulfoxide derivatives (**Fig**) were designed with the intention to study how different groups interact with PEDOT:PSS. Sulfoxide **1**, in which methyl groups in DMSO are replaced with propyl groups, is designed to examine whether the longer and more hydrophobic alkyl chains are able to modulate the conformation and aggregation of PEDOT to a greater extent (or better mixing with PSS) (**Fig. 2a**), thus affording the better TE performance. To introduce a higher molecular similarity and compatibility with a stronger van der Waals interaction between PEDOT:PSS and sulfoxide derivatives, aromatic rings were also introduced into sulfoxides **2-4** to boost the interaction between the polymer (PEDOT and PSS chains) chains and aromatic rings. Apart from the introduction of aromatic moiety in sulfoxides, several functional groups including electron-withdrawing (-NO_2) and electron-donating groups (-OH) are added into the phenyl groups. The presence of these functional groups is expected to enhance the interaction with the PEDOT and PSS phase through various weak interactions such as van der Waals force and hydrogen bonding, and in turn possibly modulate the electrical conductivity. For example, PEDOT:PSS film with only 1% sulfoxide **4** can achieved the electrical conductivity of 750 S/cm, which is almost 5 times more efficient than that of PEDOT:PSS doped with 5% DMSO. The mechanism of this enhancement was studied by using several theoretical methods. A proposed mechanism for electrical conductivity enhancement is illustrated in **Fig. 2**. This is hitherto the first example using DMSO analogues to obtain high electrical conductivity at a low sulfoxide loading.

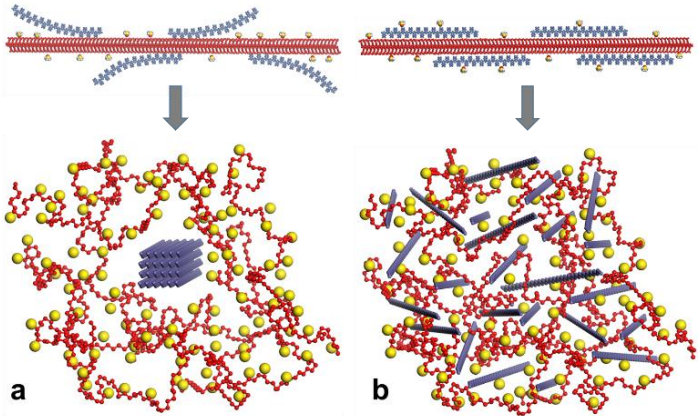

Figure 2. A proposed molecular mechanism for thermoelectric enhancement by using the sulfoxide derivatives. a) The additives (yellow) that have strong interaction with the PSS phase (red) lead to the PEDOT:PSS phase separation and PEDOT (blue) aggregation via charge screening, b) Additives that mix with both PSS and PEDOT cannot enhance thermoelectric properties.

Experimental Methods

Materials

4,4'-thiodiphenol (purity: 99%), diphenyl sulfide (purity: 98%), *meta*-Chloroperoxybenzoic acid (*m*-CPBA, purity: 76%), and dipropyl sulfide (purity: 97%) were purchased from Sigma Aldrich, Singapore. Bis(4-nitrophenyl) sulfide (purity > 99%) was purchased from Tokyo Chemical Industry (TCI), Japan. PEDOT:PSS aqueous solution (PH1000, Heraeus Clevios) was purchased from Heraeus, Germany. All other solvents, such as methylene chloride, ethanol, acetone, and distilled water were used as received without further purification.

General procedure to synthesize sulfoxides

Each sulfide (10.0 mmol) in CH_2Cl_2 (50 mL) was added to their individual reaction flask and cooled down to 0 °C using an ice bath. Then, *m*-CPBA (10.0 mmol) in CH_2Cl_2 (40 mL) was added dropwise into the sulfide solution over 30 min. The reaction mixture was then stirred for 6 h at 0 °C, and extracted consecutively with 10% NaOH (40 mL x 2), 5% HCl (40 mL), and 10% $NaHCO_3$ (40 mL). The organic layer was dried over $MgSO_4$ and filtered. The solvent was then removed through a rotary evaporator to give the respective sulfoxide.

1-(Propylsulfinyl)propane (Sulfoxide 1): Yield: 85%; ^{1}H NMR (500 MHz), *DMSO-d6*: δ 1.08 (t, *J* = 7.5 Hz, 6H), 1.76 - 1.87 (m, 4H), 2.57 - 2.63 (m, 2H), 2.71 - 2.77 (m, 2H); ^{13}C NMR (500 MHz), *DMSO-d6*: δ 13.5, 16.5, 54.3.

Sulfinyldibenzene (Sulfoxide 2): Yield: 90%; ^{1}H NMR (500 MHz), *DMSO-d6*: δ 7.48 - 7.55 (m, 6H), 7.70 - 7.73 (m, 4H); ^{13}C NMR (500 MHz), *DMSO-d6*: δ 124.1, 129.5, 131.1, 145.9.

4,4'-Sulfinylbis(nitrobenzene) (Sulfoxide 3): Yield: 78%; ^{1}H NMR (500 MHz), *DMSO-d6*: δ 8.10 (d, *J* = 9.0 Hz, 4H), 8.37 (d, *J* = 9.0 Hz, 4H); ^{13}C NMR (500 MHz), *DMSO-d6*: δ 124.8, 125.6, 149.3, 151.9.

4,4'-Sulfinyldiphenol (Sulfoxide 4): Yield: 81%; ^{1}H NMR (500 MHz), *DMSO-d6*: δ 6.86 (d, *J* = 8.5 Hz, 4H), 7.42 (d, *J* = 8.5 Hz, 4H); ^{13}C NMR (500 MHz), *DMSO-d6*: δ 116.1, 126.5, 135.5, 159.8.

Sample preparation

The glass slide was washed with water, followed by acetone, and dried under air flow. Then the glass slides were subjected to UV ozone treatment using Novascan's Ultraviolet UV Ozone Cleaners for 10 minutes to increase surface wettability. PEDOT:PSS was mixed with different concentrations of sulfoxides in ethanol. Taking a concentration of 0.1% sulfoxide as an example, PEDOT: PSS (400 mg) was first added to a 2 mL sample vial, followed by 6.7 µL of 60mg/mL sulfoxide solution at ambient temperature. The pre-mixed solution was then vortexed for 5 minutes, followed by ultra-sonication for another 15 minutes to ensure the uniform dispersion of sulfoxide into PEDOT: PSS.

Each PEDOT:PSS film was prepared by either drop-casting or spin-coating. In drop-casting, all the as-prepared solution for each respective sample was loaded onto the pre-treated glass slide, and placed on a hotplate under 80 °C for curing. Shrinkage of the film may be observed; hence the micro-pipette tip can be used to spread the sample uniformly across the glass. When no further shrinkage of the film was observed, the film was left to cure for 30 min at 80 °C. In spin-coating, the as-prepared solution for each respective sample (200 µL) was filtered using a 0.45 µm PVDF filter membrane, and spin-coated onto the pre-treated glass slide at 3,000 rpm. It was then cured under 80 °C for 30 min. Both coating methods gave very similar results in terms of electrical conductivity and Seebeck coefficient.

Characterization

^{1}H NMR and ^{13}C NMR spectra were recorded using a Bruker DRX 500-MHz NMR spectrometer in $CDCl_3$ and DMSO-d_6 solvent at room temperature. The thicknesses of the coating films were measured by the KLA Tencor P-16+ Surface Profiler. The electrical conductivity of PEDOT:PSS films was measured by Loresta-GP MCP-T600 (Mitsubishi Low Resistivity Meter) at ambient temperature. The Seebeck coefficient was measured by a custom-made system with a S A Peltier heater (298 K + ΔT) and a Peltier cooler (298 K - ΔT) used to apply and vary the temperature gradients on 2 ends of the coating film and induce a thermal voltage. Two microthermocouples (diameter 0.20 mm) were placed on the film alongside two electrodes which were connected to a Keithley 2400 source meter. The Seebeck coefficient value was then derived from a linear fit of the measured ΔV versus ΔT graph.

Computational Methods

Density Functional Theory Calculations

$$E_{mix} = \frac{1}{2}\left(Z_{ij}\left\langle E_{ij}\right\rangle_T + Z_{ji}\left\langle E_{ji}\right\rangle_T - Z_{ii}\left\langle E_{ii}\right\rangle_T - Z_{jj}\left\langle E_{jj}\right\rangle_T\right) \quad \text{Eq. 2}$$

Pairwise interaction energies between PEDOT:PSS components and sulfoxides were calculated via density functional theory (DFT) to interpret observed thermoelectric property enhancement and to understand phase organizations induced by additive treatment at the molecular level. PEDOT and PSSH trimers were used to represent components of PEDOT:PSS similar to our previous studies.[44, 45] Energetically favourable initial structure pairs with possible strong interactions were extracted from a large number of molecular configurations via statistical sampling method.[46] At least 20 lowest energy structures were determined for each pairwise interaction type. B3LYP exchange-correlation functional with DNP basis in the DMOL3 software package as well as M06-2X functional with 6-31+g(d) level by using Gaussian16.A03 software was used to determine the lowest energy structures and interaction energies to evaluate pairwise interactions. Tkatchenko-Scheffler (TS) parameters were applied for van der Waals dispersion corrections since noncovalent forces, such as hydrogen bonding and van der Waals interactions are important in additive processing of PEDOT:PSS.[47-54] Calculations were performed under implicit solvent effect by using COSMO solvent models for B3LYP functional and IEFPCM solvent models for M06-2X functional.[55, 56] Interactions of sulfoxides with negatively charged PSS^- trimer with one deprotonated monomer and positively charged radical $PEDOT^{+\cdot}$ trimer in polaron state were also calculated by using the same method to understand effect of sulfoxides on doped PSS^-:$PEDOT^+$. The pairwise interactions of sulfoxides with PEDOT:PSS components were compared with that of DMSO which is a widely used additive for thermoelectric enhancement.

Calculation of Free Energy of Solvation

Free energies of solvation were calculated for single PSS_{18} and $PEDOT_9$ oligomers solvated by DMSO and new sulfoxides, via the coupling parameter and thermodynamic integration method.[57] One of every three PSS monomers is deprotonated and charge equilibrium is provided by addition of six Na^+ cation. Initial structure of periodic cells is constructed at a density of 1 g/cm^3 with 90% w/w of sulfoxides as given for Sulfoxide **1** in the electronic supplementary information (ESI, Figure S1). The free energy of solvation was determined via a 3-step thermodynamic integration sequence after 1 ns of Molecular Dynamics (MD) simulation with isothermal–isobaric ensemble (NPT) via the Nosé-Hoover-Langevin (NHL) thermostat approach followed by cell construction and minimization. Either PSS_{18} or $PEDOT_9$ oligomer is discharged in the vacuum as the initial step, and the free energy change associated with these discharges, which is denoted as the ideal contribution to the free energy of solvation, was determined. Next, the same PEDOT and PSS oligomers were brought into contact with the solvent molecules and we obtain the van der Waals free energy change for discharged interaction. Lastly, the solvated and discharged chains are charged up in the additive environment, and the electrostatic contribution to the solvation free energy is determined. Thus, total free energy of

solvation is calculated as the sum of the contributions from the ideal term, the van der Waals and the electrostatic solvation free energies.

Calculation of Mixing Energy

The miscibility behavior of the sulfoxides with PEDOT and PSS can then be predicted based on the modified Flory-Huggins Theory.[58] The compatibility of PEDOT and PSS trimers with DMSO and sulfoxide derivatives was studied based on vacuum calculations of binary interaction energies obtained from statistical mechanics methods. Mixing energy (E_{mix}) between sulfoxides and trimers, represented as *i* and *j*, was calculated by the combination of Flory-Huggins model and COMPASS force field based molecular mechanics techniques.[59] Monte Carlo-type minimizations of a large number of cluster interactions were performed to obtain the number of neighboring components, known as coordination numbers, Z_{ij}, and the binding energies, $\langle E_{ij} \rangle$, for each pair of PEDOT:PSS and sulfoxide additives. Head and tail atoms of trimers were chosen not to be in contact so as to represent the infinitely long polymer behavior. Coordination numbers were determined by generating 10^6 clusters and the average binding energy was calculated by generating 10^8 configurations at room temperature by using the average of the weighted distribution function, P_{ij} (E) (Eq. 1).

$$\left\langle E_{ij} \right\rangle_T = \frac{\int dEEP_{ij}(E)e^{-E/RT}}{\int dEP_{ij}(E)e^{-E/RT}} \qquad \text{Eq. 1}$$

E_{mix} is defined as the difference in free energy due to interaction between the mixed PEDOT:PSS components and sulfoxide derivatives given in Eq. (2).

Results and Discussions

A series of sulfoxides **1-4** (**Fig**) were synthesized through the oxidation of the corresponding sulfides using *m*-CPBA as oxidant with high yields of 70-90%, and their chemical structures were characterized in terms of ^{1}HNMR and ^{13}C NMR spectroscopic methods. Sulfoxides **1-4** are sufficiently pure to be used as dopants for PEDOT:PSS.

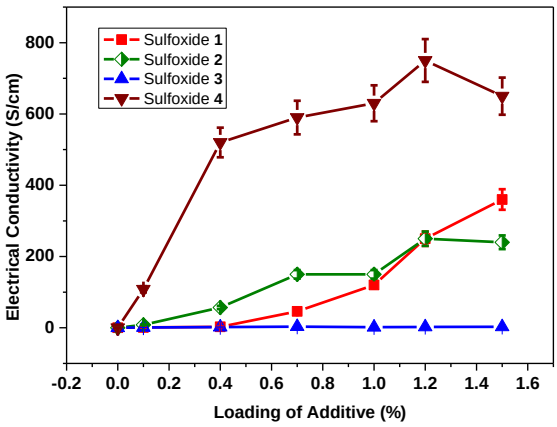

Figure 3. Electrical conductivity for the PEDOT: PSS films doped with the respective sulfoxides.

Four different sulfoxides were selected to examine how the presence of long aliphatic groups, aromatic groups and aromatic groups with electron-withdrawing or electron-donating groups affects the interaction between the sulfoxides and PEDOT:PSS. Sulfoxides were first mixed with PEDOT:PSS in different concentrations, and then coated onto the glass. The electrical conductivity of PEDOT:PSS films with four sulfoxide additives at various loadings is shown in Fig. 3. Addition of sulfoxide **1** led to increase in electrical conductivity of PEDOT:PSS film. The peak value of 280 S/cm was achieved at a loading of 1.5% sulfoxide **1**, which is not as high as that of PEDOT:PSS film with DMSO as an additive possibly due to the fact that the long alkyl chains increase the hydrophobicity of the whole molecule, leading to the poor solubility of sulfoxide **1** in aqueous solution. Sulfoxide **2** with phenyl groups exhibits a similar behaviour to sulfoxide **1**, and the electrical conductivity of PEDOT:PSS progressively increases with the increase of the concentration of sulfoxide **2** and reaches the maximum value of 207 S/cm when the sulfoxide concentration is at 1.5%. Contrary to sulfoxide **2**, sulfoxide **3** with a nitro substituent in each phenyl group does not show any tendency to cause the increase in electrical conductivity of PEDOT:PSS films when the concentration of sulfoxide increases from 0 to 1.5%. One of the reasons may arise from the low solubility of sulfoxides **2** and **3** in water as the aromatic rings are hydrophobic and thus reduce the solubility in water (**Table S1**). On the other hand, sulfoxides **2** and **3** are expected to exhibit weaker interactions with PSS components when compared to much more hydrophobic small additive DMSO molecules. In order to enhance the solubility, two hydroxy functional groups were introduced to the phenyl rings to improve the solubility of the additive and facilitate multiple interactions between PEDOT and the additive. As shown in **Fig. 3**, sulfoxide **4** with a hydroxy group in each phenyl moiety yields the highest electrical conductivity of 750 S/cm at a loading of 1.2% sulfoxide **4**.

Fig. 4 and **Fig. 5** show the respective Seebeck coefficients and power factors at the various sulfoxide loadings in PEDOT:PSS solutions. The pristine PEDOT:PSS yields a Seebeck coefficient of 22 μV/K. It is well known that Seebeck coefficient decreases with the increase in loading of DMSO.[60-63] On the contrary, changing the methyl groups in DMSO structure to other substituents (sulfoxides **1-**

4) increases the Seebeck coefficient. When sulfoxide **1** was doped in PEDOT:PSS, the Seebeck coefficient increased from 22 μV/K (pristine) to 30 μV/K at 0.7% sulfoxide loading and dropped slightly at a higher sulfoxide loading. As shown in **Fig. 5**, the power factor also reached the peak value of 21 μW m^{-1} K^{-1}. A similar trend of Seebeck coefficient was also observed for sulfoxides **2** and **3**, and the highest Seebeck coefficient was 37 μV/K at 0.7% loading and 56 μV/K at 1.2% loading, respectively. However, the corresponding highest power factor of sulfoxide doped PEDOT:PSS film was only 0.8 μW m^{-1} K^{-1} due to the extremely low electrical conductivity. PEDOT:PSS film doped with sulfoxide **4** exhibited the high Seebeck coefficient of 32 μV/K at 1% sulfoxide loading, leading to its corresponding power factor of 69 μW m^{-1} K^{-1}, which was the highest among the four sulfoxides dopants, and also much higher than that of PEDOT:PSS film doped with DMSO and without any further post-treatment.

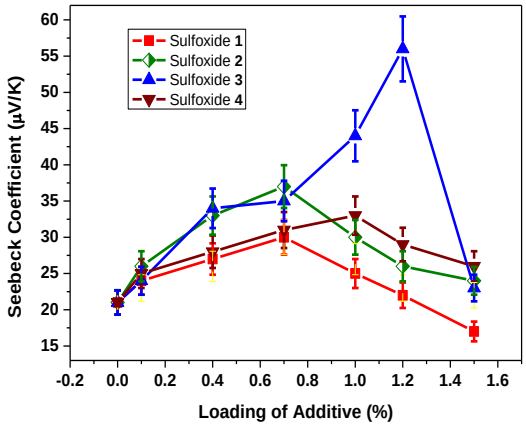

Figure 4. Seebeck coefficient of PEDOT: PSS films doped with 4 additives.

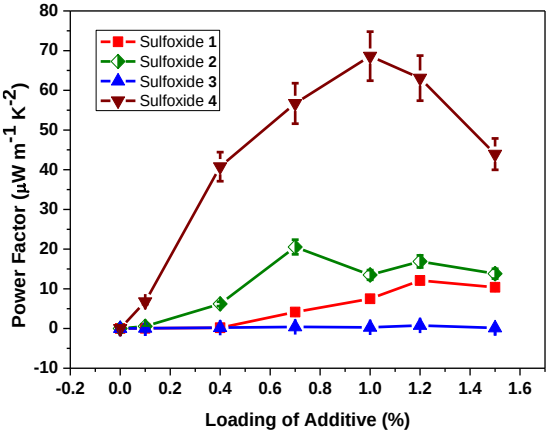

Figure 5. Power factor of PEDOT: PSS films doped with 4 additives.

Table 1. Comparison of electric properties of PEDOT:PSS film with sulfoxide **4**.

Sulfoxide **4** (%)	μ (cm^2/V·s)	n (cm^{-3})	σ (S/cm)
0	0.24±0.06	$4.02±0.12×10^{18}$	0.3±0.1
0.1	0.25±0.07	$1.25±0.10×10^{21}$	95±18
0.3	0.49±0.07	$3.11±0.10×10^{21}$	500±20
0.5	0.44±0.06	$3.38±0.25×10^{21}$	583±45
0.7	0.65±0.08	$2.26±0.27×10^{21}$	613±48
0.9	0.62±0.09	$2.91±0.23×10^{21}$	623±47
1.0	0.74±0.10	$2.46±0.28×10^{21}$	643±51

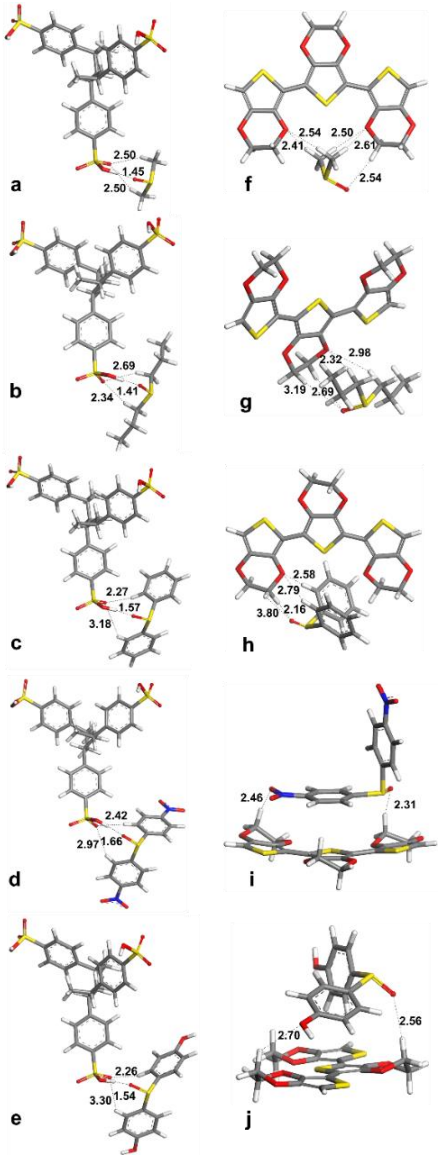

Figure 6. Lowest energy optimized structures for the pairwise interactions of a-e) PSS trimer with DMSO and sulfoxides, f-j) PEDOT trimer with DMSO and sulfoxides by B3LYP/DNP method. (carbon: grey, oxygen: red, hydrogen: white, sulfur: yellow in color)

The electric properties of PEDOT:PSS films with different concentration of the additive can be significantly enhanced through increasing the concentration of sulfoxide **4**, as determined from the Van der Pauw–Hall measurements (**Table 1**). In agreement with previously reported results,[42, 64] it is found that the pristine derived values of μ vary in the range of 0.05-0.60 cm^2/V·s. Overall, the carrier mobility improved from 0.24 to 0.74 cm^2/V·s with the increase in the concentration of sulfoxide **4** from 0 to 1.0% in PEDOT:PSS film, suggesting that the incorporation of sulfoxide **4** alters the electron-

phonon coupling to induce the increase in μ.[64, 65] In addition, carrier concentration largely increased from 4.02×10^{18} cm^{-3} for pristine PEDOT:PSS to 1.25×10^{21} cm^{-3} for PEDOT:PSS with 0.1% sulfoxide **4**, When the sulfoxide concentration is beyond 0.5%, the carrier concentration started to stabilize, which is roughly consistent with the trend of electrical conductivity.

Computational Results

Optimized structures for the lowest energy pairwise interactions of PSS and PEDOT trimer with DMSO and sulfoxide additives are given in **Fig. 6**.

In our previous studies, we reported a two-step mechanism for electrical conductivity enhancement of PEDOT:PSS by solution treatment.[44, 45] The first step lies in the reduction in the thickness of the neutral PSSH barrier to separate and release the PEDOT-rich grains. The second step is the crystallinity enhancement of PEDOT after removing the dissolved PSS shell around PEDOT. We demonstrated that the removal of insulating PSS chains around PEDOT chains by additives is the key factor for the PEDOT:PSS morphology change, leading to efficient packing of PEDOT and subsequent enhancement in its electrical conductivity. We found that hydrogen bonding between PSS-solvent should surpass PEDOT-solvent, PSS-PSS, and PEDOT-PSS interactions.

In this study, it was determined that sulfoxide group of additives forms a strong hydrogen bond with sulfonic acid group of PSS for all cases in the lowest energy structures (**Fig. 6 a-e**). Sulfoxide derivatives have an interaction with ethylene groups in the PEDOT via their sulfoxide oxygen atoms and another interaction with oxygen atoms in PEDOT via their methyl or phenyl hydrogens (**Fig. 6 f-j**). Sulfoxide **3** is the only exception where its nitro groups provide an additional interaction with the ethylene groups of PEDOT. In addition, sulfoxide **3** displays face-on interaction with PEDOT which can decrease pi-stacking and aggregation in the conducting PEDOT phase, leading to the decreased electrical conductivity, which is consistent with experimental measurement.

Interaction energies for these lowest energy PSS-sulfoxide pairs are given in **Table 2**. PSS-sulfoxide interactions are stronger than PEDOT-sulfoxide interactions for all additives except sulfoxide **3** which prefers to reside in the PEDOT phase. This theoretical observation explains why sulfoxide **3** does not lead to electrical conductivity enhancement. Same results are also valid for the second lowest energy structures and interaction energies given in the ESI (**Fig. S2**). Proton transfer from PSS to DMSO and to sulfoxide **1** were observed in M06-2X functional-based calculations which can increase PSS^- dopant ratio in the film.

Table 2. Interaction energy (in eV) between DMSO and alternative sulfoxides with PEDOT and PSS trimers calculated by two different DFT methods.

	Sulfoxide	PSS		PEDOT
B3LYP/ DNP	DMSO	-0.73	>	-0.26
	Sulfoxide **1**	-0.82	>	-0.31
	Sulfoxide **2**	-0.58	>	-0.48
	Sulfoxide **3**	**-0.39**	<	**-0.69**
	Sulfoxide **4**	-0.62	>	-0.57
M06-2X/ 6-31+g*	DMSO	-1.01 (-3.31)*	>	-0.25
	Sulfoxide **1**	-1.09 (-3.85)*	>	-0.34
	Sulfoxide **2**	-0.86	>	-0.57
	Sulfoxide **3**	**-0.70**	<	**-0.83**
	Sulfoxide **4**	-1.06	>	-0.74

**Interactions are given for PSS^--$DMSOH^+$ and PSS^--protonated Sulfoxide 1 due to the proton transfer to the additive. PSS-DMSO and PSS-Sulfoxide 1 interaction are given in parenthesis.*

The interaction energy between PSS^- anions and sulfoxide additives is significantly lower compared to the interaction energy between neutral PSS (PSSH) and sulfoxide additives (**Fig. S3**), whereas the interaction energy between $PEDOT^+$ cations in polaron form and sulfoxide additives is slightly lower compared to interaction energy between pristine PEDOT and sulfoxide additives (**Fig. S3**). We can therefore conclude that DMSO and sulfoxide derivatives (except sulfoxide **3)** affect mainly the excess neutral PSSH by removing it.

Although pairwise interactions can explain all the results for small molecules such as DMSO, DFT calculations with additional PSS trimers were performed for sulfoxide **4** which have two–OH functional groups. These –OH groups provide additional coordination and removal of PSS groups as demonstrated in Fig. 10. While DMSO and sulfoxide **4** have similar interaction energies for the pairwise interactions as given in **Table 2**, sulfoxide **4** can coordinate to two more PSS trimers via hydrogen bonds which is not possible for DMSO. The interaction energy for the PSS phase and sulfoxide **4** is much higher (**Fig. 7**), leading to better removal of insulating PSS. This justifies the relatively higher increment in the electrical conductivity for PEDOT:PSS treated with sulfoxide **4** at a much lower weight percentage compared to DMSO.

First principles calculations give us accurate description of important interactions between PEDOT:PSS components and sulfoxides. However, it only includes the interaction between the functional groups and therefore, larger scale classical calculations were carried out to analyse miscibility and compatibility via the mixing energies and solvation free energies (**Table 3**).

All mixing energies have negative values for PSS and positive values for PEDOT which explain why the PSS ratio in the film decreases and PEDOT phase becomes larger after solution processing. Stronger interaction with the PSS phase provided by additional –OH groups and structural similarity leads to the better mixing of PSS with sulfoxide **4**.

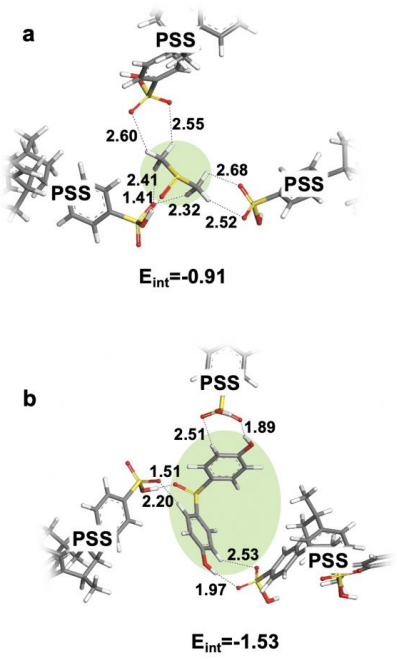

Figure 7. Lowest energy optimized structures and interaction energies of three PSS trimer with the sulfoxides (in green): a) DMSO and b) sulfoxide **4**. Full image is available in **Fig. S4**.

Table 3. Mixing energy (E_{mix}) and free energy of solvation (ΔE_{sol}) calculated for PEDOT and PSS with DMSO and alternative additives.

i	*j*	E_{mix} (kcal/mol)	ΔE_{sol} (kcal/mol)
PSS	DMSO	-37.32	-316.17
	Sulfoxide **1**	-39.26	-239.63
	Sulfoxide **2**	-27.57	-174.50
	Sulfoxide **3**	-29.51	-131.47
	Sulfoxide **4**	-51.41	-227.03
PEDOT	DMSO	13.94	-54.45
	Sulfoxide **1**	10.10	-43.16
	Sulfoxide **2**	6.35	-29.48
	Sulfoxide **3**	1.46	-38.81
	Sulfoxide **4**	7.93	-16.81

Another important finding is that the mixing energy of PEDOT with sulfoxide **3** has the least positive value. This close-to-zero mixing energy for PEDOT-sulfoxide **3** indicates the potential sulfoxide **3** residue in the PEDOT phase to disrupt aggregation and impeding electrical conductivity enhancement.

In similar context, solvation free energies of PSS chain by all sulfoxides are significantly higher compared to the solvation free energies of PEDOT chain by the same sulfoxides. DMSO and sulfoxide **1** have the highest solvation free energies for both PSS and PEDOT mainly due to their small sizes and number of solvent molecules. While 398 DMSO molecules were used for simulating a 90% w/w ratio, only 133 sulfoxide **4** molecules were required in the periodic cells of same size. Comparing the solvation free energies of PEDOT and PSS by sulfoxides **2, 3**, and **4** with similar molecular sizes; sulfoxide **4** has the highest solvation free energy of PSS and lowest solvation free energy of PEDOT, whereas sulfoxide **3** has the highest solvation free energy of PEDOT and lowest solvation free energy of PSS.

DFT calculations, mixing energies, and solvation free energies have shown that PSS-sulfoxide interactions should be the dominant interaction among all pairwise interactions in PEDOT:PSS-sulfoxide mixture for electrical conductivity enhancement. Sulfoxide **4** shows comparable solvation effects as DMSO for inducing phase separation in PEDOT-PSS at much lower loading. It was revealed that sulfoxide **4** possesses additional interaction with PSS phase in PEDOT:PSS, leading to enhanced thermoelectric performance, while Sulfoxide **3** which has relatively stronger interaction with conducting PEDOT phase solvate PEDOT chains disrupts pi stacking, leading to low and almost constant thermoelectric performance with Sulfoxide **3** loading.

Conclusion

In summary, treatment of PEDOT:PSS with sulfoxides was studied experimentally as well as through multiscale molecular modelling. Experimental results demonstrated that sulfoxides behaved differently, and the substituents of sulfoxides have a substantial effect on the thermoelectric properties in particular electrical conductivity at a low loading. Sulfoxides with longer aliphatic propyl chains and larger phenyl groups than methyl group in DMSO resulted in moderate increase in electrical conductivity up to a few hundred S/cm at a loading of 1.5%. Nitro-substitution in *para*-phenyl groups of sulfoxide, however, did not cause any increment in electrical conductivity. On the contrary to electron-withdrawing groups, electron-donating hydroxy-substitution in sulfoxide improved the electrical conductivity up to 750 S/cm, giving a highest power factor of 69 $\mu W\ m^{-1}\ K^{-2}$ amongst all sulfoxides-doped PEDOT:PSS films. The details for the mechanism behind the experimental observations were investigated by different simulation tools. The potential interactions between the sulfoxide additives and PEDOT and PSS were calculated, revealing that sulfoxide **4** possessed additional interaction with the PSS phase in PEDOT:PSS, leading to enhanced thermoelectric performance. In contrast, sulfoxide **3** exhibited strong interaction with the PEDOT phase instead, disrupted electrical conductivity and hence did not enhance the electrical conductivity. Our findings demonstrated distinct mechanisms of different sulfoxides as additives of PEDOT:PSS to improve the thermoelectric performance. Moreover, this work would provide a model example for general strategies to design and synthesize new high performance additive for thermoelectric PEDOT:PSS.

Acknowledgement

The authors would like to acknowledge the financial support from Industry Alignment Fund, Pharos "Hybrid thermoelectric materials for ambient applications" Programme (Grant No. 1527200019 & 1527200021 & 1527200024), A*STAR, Singapore. Computational resources are provided by the National Supercomputing Centre Singapore (NSCC) and A*STAR Computational Resource Centre (A*CRC).

Conflicts of interest

"There are no conflicts to declare".

Notes and references

1. J. P. Heremans, M. S. Dresselhaus, L. E. Bell and D. T. Morelli, *Nat. Nanotechnol.*, 2013, **8**, 471.
2. J. R. Sootsman, D. Y. Chung and M. G. Kanatzidis, *Angew. Chem. Int. Ed.*, 2009, **48**, 8616-8639.
3. Y. Lan, A. J. Minnich, G. Chen and Z. Ren, *Adv. Funct. Mater.*, 2010, **20**, 357-376.
4. M. Zebarjadi, K. Esfarjani, M. Dresselhaus, Z. Ren and G. Chen, *Energy Environ. Sci.*, 2012, **5**, 5147-5162.
5. Q. Yao, L. Chen, W. Zhang, S. Liufu and X. Chen, *Acs Nano*, 2010, **4**, 2445-2451.
6. R. Venkatasubramanian, E. Siivola, T. Colpitts and B. O'quinn, *Nat.*, 2001, **413**, 597-602.
7. Y. Zheng, Y. Luo, C. Du, B. Zhu, Q. Liang, H. H. Hng, K. Hippalgaonkar, J. Xu and Q. Yan, *Mater. Chem. Front.*, 2017, **1**, 2457-2473.
8. Y. Luo, C. Du, Q. Liang, Y. Zheng, B. Zhu, H. Hu, K. A. Khor, J. Xu, Q. Yan and M. G. Kanatzidis, *Small*, 2018, **14**, 1803092.
9. Z.-Z. Luo, S. Cai, S. Hao, T. P. Bailey, X. Su, I. Spanopoulos, I. Hadar, G. Tan, Y. Luo and J. Xu, *J. Am. Chem. Soc.*, 2019, **141**, 16169-16177.
10. X. Yong, W. Shi, G. Wu, S. S. Goh, S. Bai, J.-W. Xu, J.-S. Wang and S.-W. Yang, *J. Mater. Chem. A*, 2018, **6**, 19757-19766.
11. Y. Luo, Y. Zheng, Z. Luo, S. Hao, C. Du, Q. Liang, Z. Li, K. A. Khor, K. Hippalgaonkar and J. Xu, *Adv. Energy Mater.*, 2018, **8**, 1702167.
12. T. Harman, P. Taylor, M. Walsh and B. LaForge, *Science*, 2002, **297**, 2229-2232.
13. X. Wang, H. Lee, Y. Lan, G. Zhu, G. Joshi, D. Wang, J. Yang, A. Muto, M. Tang and J. Klatsky, *Appl. Phys. Lett.*, 2008, **93**, 193121.
14. M. Culebras, C. M. Gómez and A. Cantarero, *Materials*, 2014, **7**, 6701-6732.
15. B. Zhang, J. Sun, H. Katz, F. Fang and R. Opila, *ACS Appl. Mater. Interfaces*, 2010, **2**, 3170-3178.
16. C. Yoon, M. Reghu, D. Moses, Y. Cao and A. Heeger, *Synth. Met.*, 1995, **69**, 255-258.
17. N. Mateeva, H. Niculescu, J. Schlenoff and L. Testardi, *J. Appl. Phys.*, 1998, **83**, 3111-3117.
18. A. G. MacDiarmid, *Synth. Met.*, 2001, **125**, 11-22.
19. Y. Hu, H. Shi, H. Song, C. Liu, J. Xu, L. Zhang and Q. Jiang, *Synth. Met.*, 2013, **181**, 23-26.
20. N. Kemp, A. Kaiser, C. J. Liu, B. Chapman, O. Mercier, A. Carr, H. Trodahl, R. Buckley, A. Partridge and J. Lee, *J. Polym. Sci., Part B: Polym. Phys.*, 1999, **37**, 953-960.
21. H. Kaneko, T. Ishiguro, A. Takahashi and J. Tsukamoto, *Synth. Met.*, 1993, **57**, 4900-4905.
22. Z. Fan and J. Ouyang, *Adv. Electron. Mater.*, 2019, **5**, 1800769.
23. Y. Zheng, H. Zeng, Q. Zhu and J. Xu, *J. Mater. Chem. C*, 2018, **6**, 8858-8873.
24. X. Wang, A. K. K. Kyaw, C. Yin, F. Wang, Q. Zhu, T. Tang, P. I. Yee and J. Xu, *RSC Adv.*, 2018, **8**, 18334-18340.
25. A. K. K. Kyaw, T. A. Yemata, X. Wang, S. L. Lim, W. S. Chin, K. Hippalgaonkar and J. Xu, *Macromol. Mater. Eng.*, 2018, **303**, 1700429.
26. T. A. Yemata, A. K. K. Kyaw, Y. Zheng, X. Wang, Q. Zhu, W. S. Chin and J. Xu, *Polym. Int.*, 2020, **69**, 84-92.
27. J. Xu, Q. Zhu, E. Yildirim, X. Wang, X. Y. D. S. Soo, Y. Zheng, T. L. Tan, G. Wu and S.-W. Yang, *Front. Chem.*, 2019, **7**, 783.
28. T. A. Yemata, Y. Zheng, A. K. K. Kyaw, X. Wang, J. Song, W. S. Chin and J. Xu, *Front. Chem.*, 2020, **7**, 870.
29. T. A. Yemata, Y. Zheng, A. K. K. Kyaw, X. Wang, J. Song, W. S. Chin and J. Xu, *RSC Adv.*, 2020, **10**, 1786-1792.
30. E. S. Cho, N. E. Coates, J. D. Forster, A. M. Ruminski, B. Russ, A. Sahu, N. C. Su, F. Yang and J. J. Urban, *Adv. Mater.*, 2015, **27**, 5744-5752.
31. G. O. Park, J. W. Roh, J. Kim, K. Y. Lee, B. Jang, K. H. Lee and W. Lee, *Thin Solid Films*, 2014, **566**, 14-18.
32. G. P. Moriarty, K. Briggs, B. Stevens, C. Yu and J. C. Grunlan, *Energy Technol.*, 2013, **1**, 265-272.
33. K. Xu, G. Chen and D. Qiu, *J. Mater. Chem. A*, 2013, **1**, 12395-12399.
34. P. Kumar, E. W. Zaia, E. Yildirim, D. M. Repaka, S.-W. Yang, J. J. Urban and K. Hippalgaonkar, *Nat. Commun.*, 2018, **9**, 1-10.
35. K. Kato, H. Hagino and K. Miyazaki, *J. Electron. Mater.*, 2013, **42**, 1313-1318.
36. C. Liu, F. Jiang, M. Huang, B. Lu, R. Yue and J. Xu, *J. Electron. Mater.*, 2011, **40**, 948-952.
37. J. Wu, Y. Sun, W.-B. Pei, L. Huang, W. Xu and Q. Zhang, *Synth. Met.*, 2014, **196**, 173-177.
38. Q. Wei, M. Mukaida, K. Kirihara, Y. Naitoh and T. Ishida, *Materials*, 2015, **8**, 732-750.
39. B. T. McGrail, A. Sehirlioglu and E. Pentzer, *Angew. Chem. Int. Ed.*, 2015, **54**, 1710-1723.
40. M. Culebras, C. Gómez and A. Cantarero, *J. Mater. Chem. A*, 2014, **2**, 10109-10115.
41. H. Park, S. H. Lee, F. S. Kim, H. H. Choi, I. W. Cheong and J. H. Kim, *J. Mater. Chem. A*, 2014, **2**, 6532-6539.
42. Z. Fan, P. Li, D. Du and J. Ouyang, *Adv. Energy Mater.*, 2017, **7**, 1602116.
43. G.-H. Kim, L. Shao, K. Zhang and K. P. Pipe, *Nat. Mater.*, 2013, **12**, 719-723.
44. E. Yildirim, G. Wu, X. Yong, T. L. Tan, Q. Zhu, J. Xu, J. Ouyang, J.-S. Wang and S.-W. Yang, *J. Mater. Chem. C*, 2018, **6**, 5122-5131.
45. E. Yildirim, Q. Zhu, G. Wu, T. L. Tan, J. Xu and S.-W. Yang, *J. Phys. Chem. C*, 2019, **123**, 9745-9755.
46. M. Blanco, *J. Comput. Chem*, 1991, **12**, 237-247.
47. B. Delley, *J. Chem. Phys.*, 2000, **113**, 7756-7764.
48. M. Frisch, G. Trucks, H. Schlegel, G. Scuseria, M. Robb, J. Cheeseman, G. Scalmani, V. Barone, G. Petersson and H. Nakatsuji, *Journal*.
49. D. S. BIOVIA, 2018.
50. A. D. Becke, *J. Chem. Phys*, 1993, **98**, 5648-5652.
51. C. Lee, W. Yang and R. Parr, *Phys. Rev, vol. B*, 1988, **37**, 785-789.
52. P. J. Stephens, F. Devlin, C. Chabalowski and M. J. Frisch, *J. Phys. Chem.*, 1994, **98**, 11623-11627.
53. Y. Zhao and D. G. Truhlar, *Theor. Chem. Acc.*, 2008, **120**, 215-241.
54. A. Tkatchenko and M. Scheffler, *Phys. Rev. Lett.*, 2009, **102**, 073005.

55. A. Klamt and G. Schüürmann, *Journal of the Chemical Society, Perkin Transactions 2*, 1993, 799-805.
56. B. Mennucci, E. Cances and J. Tomasi, *The Journal of Physical Chemistry B*, 1997, **101**, 10506-10517.
57. T. Steinbrecher, I. Joung and D. A. Case, *J. Comput. Chem*, 2011, **32**, 3253-3263.
58. C. F. Fan, B. D. Olafson, M. Blanco and S. L. Hsu, *Macromolecules*, 1992, **25**, 3667-3676.
59. J. Sun, R. Haunschild, B. Xiao, I. W. Bulik, G. E. Scuseria and J. P. Perdew, *J. Chem. Phys.*, 2013, **138**, 044113.
60. J. Feng-Xing, X. Jing-Kun, L. Bao-Yang, X. Yu, H. Rong-Jin and L. Lai-Feng, *Chinese Physics Letters*, 2008, **25**, 2202.
61. R. Yue, S. Chen, C. Liu, B. Lu, J. Xu, J. Wang and G. Liu, *J. Solid State Electrochem.*, 2012, **16**, 117-126.
62. K.-C. Chang, M.-S. Jeng, C.-C. Yang, Y.-W. Chou, S.-K. Wu, M. A. Thomas and Y.-C. Peng, *J. Electron. Mater.*, 2009, **38**, 1182-1188.
63. M. Scholdt, H. Do, J. Lang, A. Gall, A. Colsmann, U. Lemmer, J. D. Koenig, M. Winkler and H. Boettner, *J. Electron. Mater.*, 2010, **39**, 1589-1592.
64. Y.-J. Lin, W.-S. Ni and J.-Y. Lee, *J. Appl. Phys.*, 2015, **117**, 215501.
65. D. A. Mengistie, C.-H. Chen, K. M. Boopathi, F. W. Pranoto, L.-J. Li and C.-W. Chu, *ACS Appl. Mater. Interfaces*, 2015, **7**, 94-100.